Hydrology, Environment (Pedology)

New characterization aspects of carbonate accumulation horizons in Chalky Champagne (NE of the Paris Basin, France)

Damien Linoir *, Céline Thomachot-Schneider, Maxime Gommeaux, Gilles Fronteau, Vincent Barbin

EA3795 GEGENAA, Université de Reims Champagne-Ardenne, Centre de recherches en environnement et agronomie, 2, esplanade Roland-Garros, 51100 Reims, France

A B S T R A C T

The soil profiles of the Champagne area (NE of Paris Basin, France) occasionally show carbonate accumulation horizons (CAHs). From the top to the bottom, these soil profiles include a rendic leptosol horizon, a Quaternary cryoturbated paleosol (QCP), and a chalky substratum. The CAHs are located in the top part of the QCP. This study is aimed at highlighting the specific characteristics of CAHs compared to other soil profile horizons using geophysics, geochemistry, micromorphology, and mercury injection porosimetry. It is the first essential step for understanding the impact of CAHs on water transfers into the Champagne soil profiles. Our analyses show that Champagne CAHs are not systematically characterized by a typical induration unlike generally put forward in the regional literature. They are more porous and heterogeneous than their parent material (QCP). Carbonate accumulation horizons are also characterized by singular colorimetric parameters that are linked to their geochemical specific content, even if they bear a signature of the initial QCP before the pedogenic modification.

1. Introduction

Pedogenic carbonate accumulation horizons (CAHs) are typical features of soil formation in arid and semiarid environments, and occur in a variety of forms (Wright and Tucker, 1991). They are mainly formed under Mediterranean to subarid conditions (Alonso-Zarza, 1999; Alonso-Zarza and Wright, 2010; Hamidi et al., 2001). However, CAHs also occur in the various climatic conditions of tropical (Goudie, 1973), subdesert (Schlesinger, 1985), Arctic (Lauriol and Clark, 1999), and semicontinental (Loisy et al., 1999) environments.

In the Paris Basin, several French authors found pedogenetic CAHs (Bruand et al., 1997; Chéry et al., 1999; Hommeril et al., 1974; Nicoullaud et al., 1995; Ould and Bruand, 1993). They are located in the upper part of a Quaternary superficial formation originating from cryoturbation of the Cretaceous chalky substratum under periglacial climate (Allouc and Le Roux, 1995, 2000; Ballif, 1994; Ballif et al., 1995; Bouttemy, 1966; Laurain et al., 1981; Loisy, 1997; Loisy and Pascal, 1998; Loisy et al., 1999; Spanneut, 1997) and immediately under the organomineral horizon. These Champagne-Ardenne CAHs appear as conglomerates of cryoclastic chalky sands and gravels coated with limey-clayey silts. They are 5–20 cm thick, with occasionally a slab detachment, and they seem, sometimes, lighter colored than the cryoturbated paleosol.

Previous studies showed that the formation of the Champagne CAHs began at the end of the Lateglacial (14,000

* Corresponding author.
E-mail address: damien.linoir@yahoo.fr (D. Linoir).

years BP) under a periglacial climate and that it continues in the current period under temperate and continental climates (Durand, 1979, 1980; Loisy, 1997; Loisy and Pascal, 1998). However, if these studies give descriptions of CAHs, they only focus on the carbonate CAHs and do not take into account the QCP, which is considered as the CAH host level (Loisy, 1997; Loisy et al., 1999).

The present study aims at highlighting the characteristics specific to the CAHs by comparing them to other soil profile horizons and particularly to QCP, in which they may be formed. It is based not only on in situ analyses (dynamic penetrometry and colorimetric tests), but also on micromorphological observation (optical and SEM), geochemical content study, and mercury injection porosimetry. In addition to allowing the establishment of a precise and specific CAH definition, this characterization will allow a better understanding of the CAHs impact on water transfers within soil profiles or lateral fluxes (Banwart et al., 2012), or the lack of carbon sequestration horizon (Robert and Saugier, 2003), which are particularly vital in this region where the chalk aquifer is submitted to high agroindustrial pressures.

2. Materials and methods

2.1. Study site

The study site, a former Santonian chalk quarry, is located in Chalky Champagne, at Mont du Ménil (on the commune of Aussonce: 49°21′38″ N, 4°18′08″ E), about twenty kilometers north-east of the city of Reims (Northeast of the Paris Basin) (Fig. 1). This site offers good conditions for observation and sampling of CAHs and of other soil profile horizons. The study site is located at the top of a slope, under a vegetation cover containing herbaceous plants and shrubs.

The studied profile extends over 4 linear meters at the top of a slope (Fig. 1). It can be divided, from the bottom to the top, into four formations, which are: (1) a massive chalk (C) covered with (2) a Quaternary cryoturbated paleosol (QCP), (3) a carbonate accumulation horizon (CAH), and (4) a rendic leptosol (A) following the FAO WRB classification (2006), with a thickness ranging from 20 to 45 cm (Fig. 1) and high organic matter content. The rendic leptosol is hereafter considered as a single formation, notwithstanding the different horizons that might be described therein.

The QCP is a truncated polygonal paleosol formed by chalk alteration under periglacial climate up to 14,000 years BP (Ballantyne and Harris, 1994; Ballif et al., 1995). Its composition results from the fragmentation of chalk material, the formation of pocket-shaped structures by cryoclasty and cryosuction phenomena (Laurain et al., 1995; Murton et al., 2003). The thickness of the cryoturbated material on the site varies from 70 to 120 cm and its upper limit with the CAH is very clear (Fig. 1).

A description of the CAH found at this site is given by Loisy and Pascal (1998) and Loisy et al. (1999). This CAH results from calcite impregnation of the upper part of the QCP. The thickness of the CAH varies from 20 cm in the northwestern zone to 5 cm in the southeastern zone (Fig. 1). The morphology of this horizon also varies along the profile. It is mostly homogeneous and massive in the northwestern zone and shows a slab detachment in the southeastern zone. The upper limit of this CAH with the rendic leptosol is also well defined.
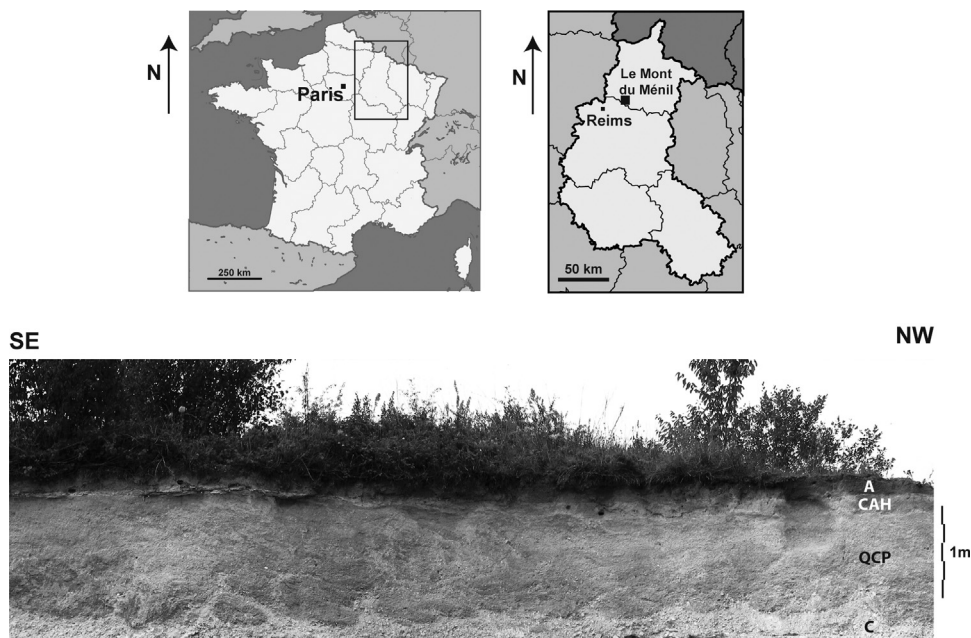

Fig. 1. Location of the studied site: the Mont du Ménil (commune of Aussonce, Champagne-Ardenne region) and studied profile photography. A, rendosol A horizon; CAH, carbonate accumulation horizon; QCP, quaternary cryoturbated paleosol; C, chalk.

2.2. Colorimetry

On the field, CAHs sometimes seem to differ from the QCP, showing a lighter color. Colorimetry tests were carried out in order to propose field colorimetric measurements as a CAH recognition technique. Twenty measurements of colorimetry were taken at random on each horizon of the entire profile (A, CAH, QCP, and C). No subdivision was noticed in the rendic leptosol.

We chose the $L^*a^*b^*$ color system, which quantifies a color by a light intensity parameter, L^*, and two other parameters, a^* and b^*, corresponding respectively to color variation on green/red and blue/yellow axes.

In this color system, the calculation of the Euclidean distance allows one to obtain the global color difference between two objects, generally noted as ΔE^* (Moreau, 2008). The calculation of ΔE^* is performed according to the Eq. (1):

$$\Delta E_{*c1:c2} = \sqrt{((L_{*c1}-L_{*c2})^2 + (a_{*c1}-a_{*c2})^2 + (b_{*c1}-b_{*c2})^2)} \tag{1}$$

where L^*_{c1}, a^*_{c1} and b^*_{c1} are the coordinates of the first color and L^*_{c2}, a^*_{c2} and b^*_{c2} are the coordinates of the second color in the $L^*a^*b^*$ color system. Moreau (2008) indicates that a color difference ≤ 3 is not discernible to the naked eye.

2.3. Geochemical overview

Major element composition was analyzed by ICP-AES and the results are given in weight percentage of oxide. The total carbonate content was obtained by using a calcimeter (Bernard type), and the results were expressed in $g\,kg^{-1}$. The geochemical study was conducted on 17 samples taken from the soil profile: four for the rendic leptosol, five for the CAH, six for the QCP, and two for the chalk. Each sample weighed 10 g.

2.4. Dynamic cone penetrometry

Dynamic cone penetrometry was used in order to determine first the strength of the different horizons of the soil profile, and second, to validate or not the characterization of Champagne-Ardenne CAHs by higher resistance compared to the other horizons. Five profiles were tested along the 4 linear meters of the studied area.

The device consists of a drill string provided with a conical penetrating tip. Penetration into the soil is done by manual pounding of a strain gauge ram head by a hammer ballasted with lead (Sanglerat, 2012). For each hammer blow, the dialog terminal calculates the tip resistance Q_d (MPa) using the Dutch equation (Sanglerat, 2012) (2):

$$Q_d = (1/A) \times (E/e) \times (1/(1 + (P/m)))$$
$$= (m^2 v^2)/(Ae(m + P)) \tag{2}$$

where m is the hammering mass ($kg\,m^2\,s^{-2}$), v is the hammering velocity ($m\,s^{-1}$), A is the tip section (m^2), e is the drill string penetration (m), and P is the hammered mass (kg).

2.5. Micromorphology

Thin sections (4.5 cm vertical by 3 cm horizontal) were carried out in quincunx along the blocks sampled from the profiles (10 thin sections for 20 cm of the vertical profile). Micromorphological analyses were performed both on fragments and on thin sections of the CAH, QCP, and chalk. Observations were performed by using a polarizing petrographic microscope (Olympus BX51). A scanning electron microscope (Hitachi TM-1000 Table Top) equipped with an energy-dispersive X-ray spectrometer was also used in back-scattered electron mode. Observations were carried out with a 15-kV accelerating voltage and a 6-mm working distance.

2.6. Mercury injection porosimetry

Mercury intrusion porosimetry (MIP) quantifies both the value of total porosity N_{Hg} and the pore access distribution in a porous material (Cérépi et al., 2009; Gallé, 2001; Hildenbrand and Urai, 2003; Yven et al., 2007). The relationship between the applied mercury capillary pressures and the pore access radius is given by the Young–Laplace equation:

$$P = -(2\sigma|\cos\theta|)/r \tag{3}$$

where P is the capillary pressure (Pa), σ the mercury surface tension ($0.485\,N\,m^{-1}$), θ the contact angle between mercury and the contact surface ($140°$), and r the pore access radius (m). According to this relationship, each applied pressure corresponds to a pore access radius.

Analyses were carried out with a Micromeritics Auto-Pores IV 9500 apparatus. The measured pore access radii ranged from 180 μm (0.004 MPa) to 0.003 μm (274 MPa).

The soil pores' dispersion is characterized by the scatter coefficient C_d:

$$C_d = (P_{80}-P_{20})/P_{50} \tag{4}$$

where P_{20}, P_{50}, and P_{80} are the intrusion pressures, which correspond respectively to the filling of 20%, 50%, and 80% of the porous network (Wardlaw et al., 1988). A value of C_d lower than 1 corresponds to a distribution centered around a pore access radius value, while a $C_d > 1$ characterizes a moderate to high dispersion in the distribution of the values of the pore access radius (Remy, 1993; Wardlaw et al., 1988).

MIP analyses were carried out on 1.5-cm^3 samples systematically collected every 2 cm along the soil profile.

3. Results

3.1. Colorimetric characterization

Our colorimetry measurements (Table 1) show that the color is darker (L^* values) in CAH than in chalk (66.2 ± 6.4 against 89.9 ± 0.8). On the contrary, the CAH color is clearly lighter than those of the rendic leptosol and of QCP (respectively 50.5 ± 5.6 and 62.5 ± 2.6). However, the L^* difference between CAH and QCP is fairly low. The variation of a^* value between the different horizons is relatively low.

Table 1

Values of color parameter in the $L^*a^*b^*$ obtained for the different studied horizons and ΔE^* between CAHs/chalk and other horizons.

	L^*	a^*	b^*	ΔE^*_{CAH}	ΔE^*_{Chalk}
A	50.5 ± 5.6	4.1 ± 0.7	12.0 ± 0.5	13.92	38.18
CAH	66.2 ± 6.4	2.1 ± 0.7	10.2 ± 1.7		24.35
QCP	62.5 ± 2.6	3.0 ± 0.4	15.8 ± 1.1	8.64	29.61
Chalk	89.9 ± 0.8	0.1 ± 0.1	7.6 ± 0.6	24.35	

They indicate that CAH tints present less pronounced red components than the rendic leptosol and the QCP (2.1 ± 0.7 against 4.1 ± 0.7 and 3.0 ± 0.4). However, CAH tints exhibit more red components than the chalk (0.1 ± 0.1). Observation of b^* values shows that CAH are less yellow than the rendic leptosol and QCPs (10.2 ± 1.7 against 12.0 ± 0.5 and 15.8 ± 1.1). CAH tints present more pronounced yellow components than chalk (7.6 ± 0.6).

The ΔE^* calculated values (Table 1) first indicate that each horizon of the soil profile may be distinguishable from the others to the naked eye ($\Delta E^* > 3$). Most important color differences ($\Delta E^* > 24$) are observed when chalk samples are compared to other horizons. The color difference is low between CAH and QCP ($\Delta E^* = 8.64$) and mean between CAHs and the rendic leptosol ($\Delta E^* = 13.92$).

3.2. Geochemical parameters

The higher $CaCO_3$ values (Fig. 2) are observed for the CAH ($885.3 \pm 21.0 \, g \, kg^{-1}$) whereas the lower $CaCO_3$ values appear for the QCP ($826.7 \pm 15.1 \, g \, kg^{-1}$). The $CaCO_3$ content is relatively high and low, respectively in the chalk ($880.0 \pm 0.0 \, g \, kg^{-1}$) and in the rendic leptosol ($836.0 \pm 4.0 \, g \, kg^{-1}$).

The most important part of the major oxides present within the soil profile horizons is represented by CaO (about 80% in the rendic leptosol and QCP, about 90% in the CAH and 97% in the chalk). In the rest of the major oxides, the major part is represented by SiO_2 (14.3%, 11.7%, 6.4%, and 1.7% respectively for QCP, rendic leptosol, CAH, and chalk). Al_2O_3 represents 3.2%, 2.7%, 2.2%, and 0.7% of the rendic leptosol, QCP, CAH, and chalk, respectively, whereas 1.3%, 1.1%, 1.0%, and 0.3% of the rendic leptosol, QCP, CAH, and chalk, respectively, are represented by Fe_2O_3.

3.3. Vertical resistance profile

In thin CAH typical profiles, the rendic leptosol exhibited low tip resistance values ranging between 0.2 and 2 MPa, and while the CAH was not clearly defined, it showed the same tip resistance values as the QCP (between 2 and 9 MPa) (Fig. 2). In a thick CAH typical profile, the tip resistance values started to increase in the basal part of the rendic leptosol (3.5 MPa against <1 for the top part of the rendic leptosol) (Fig. 2). The CAH exhibited the same tip resistance values as the basal part of the rendic leptosol. The beginning of the QCP was characterized by an increase in the tip resistance values (8–10 MPa) (Fig. 2).

Even though the limit between the rendic leptosol and the CAHs was very clear on the field (color change), no clearly defined limit allows us to clearly distinguish the different horizons of the soil profile by dynamic penetrometry.
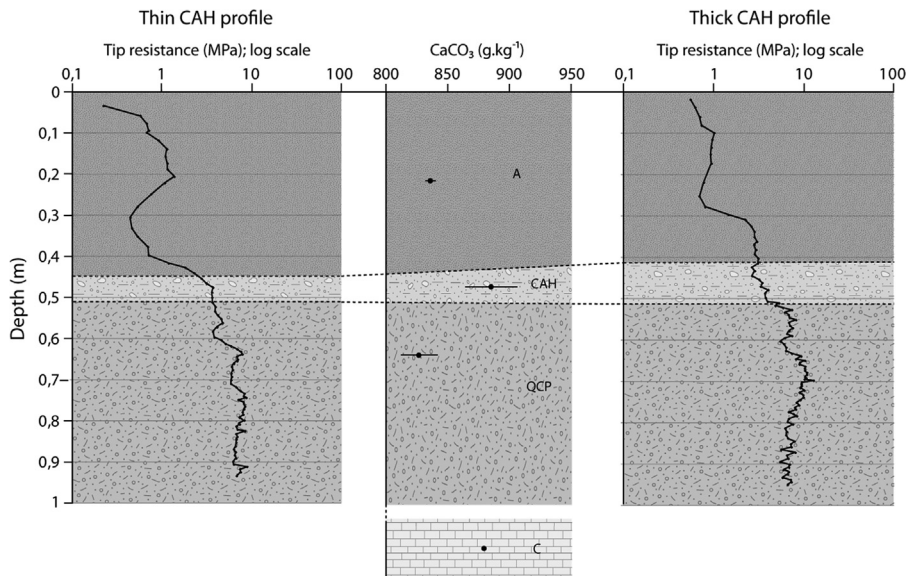

Fig. 2. Penetrometric characteristics of the thin and thick CAH soil profile and $CaCO_3$ mean contents (and standard deviations) of the different horizons of the soil profile.
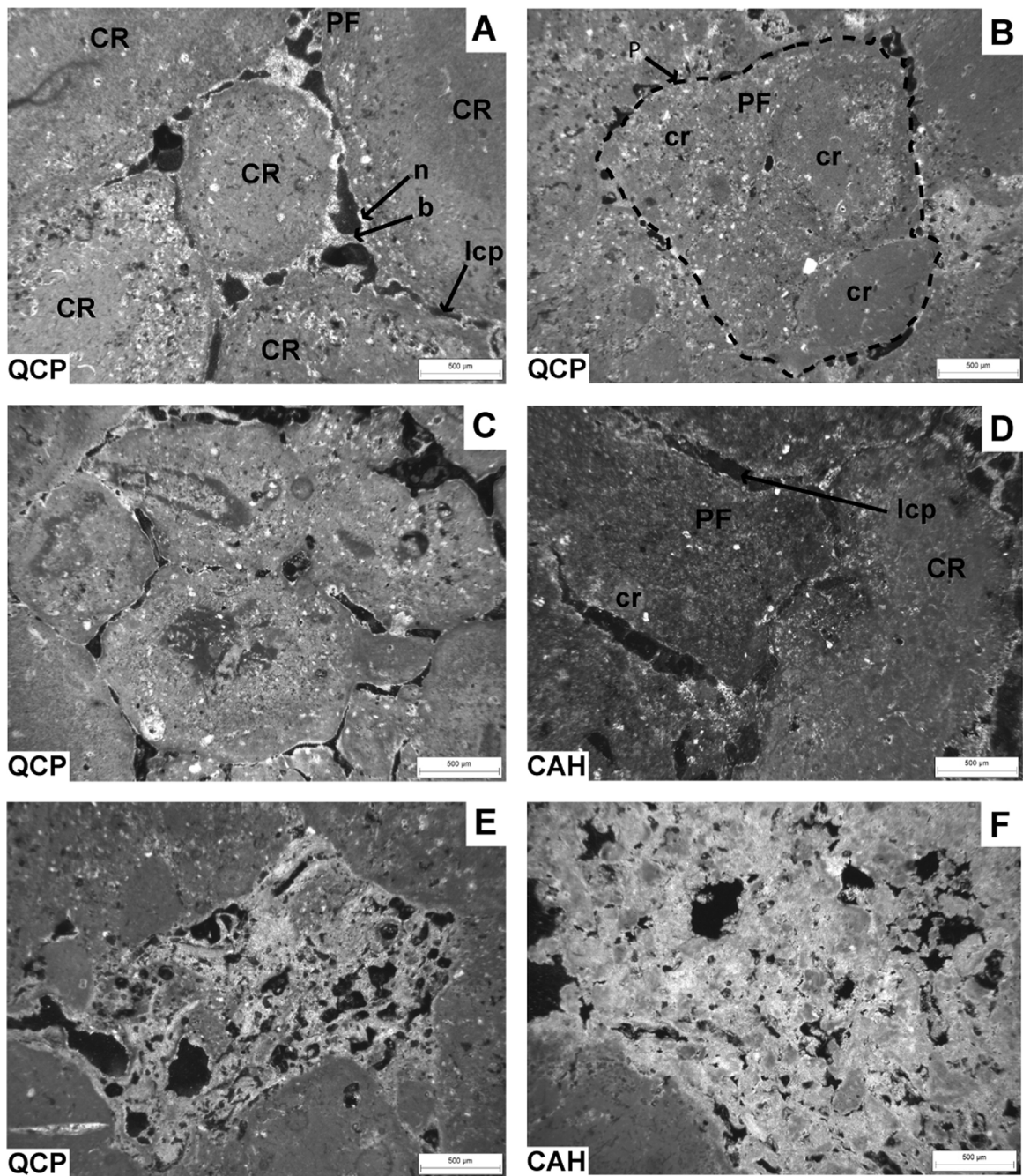
Fig. 3. Microstructures of the CAH and the QCP in thin sections (polarized light). Views of A: large chalk cryoclast (CR) coated with a thin layer of plasmic fabric (PF) and calcite needles (n) that can form arch-shaped bridges (b), interpedal curved planes (Icp) within QCP; B: a typical spheroidal to blocky ped (P) containing small cryoclast occurrences (cr) within QCP; C: typical QCP interpedal curved planes (Icp) presenting numerous constrictions; D: typical larger CAH interpedal curved planes (Icp) generally well connected; E: star-shaped vugh observed in QCP; F: wide star-shaped vugh that exhibits a complexity of structure observed in the CAH.

3.4. Micromorphological characterization

SEM observations show that chalk has a conventional composition. It contains coccoliths fragments, which fill the spaces between whole or slightly dismantled coccoliths. It also contains some quartz grains and clay minerals. However, a very thin and homogenous porosity (Ø of about 0.7 μm) can be observable between all these components.

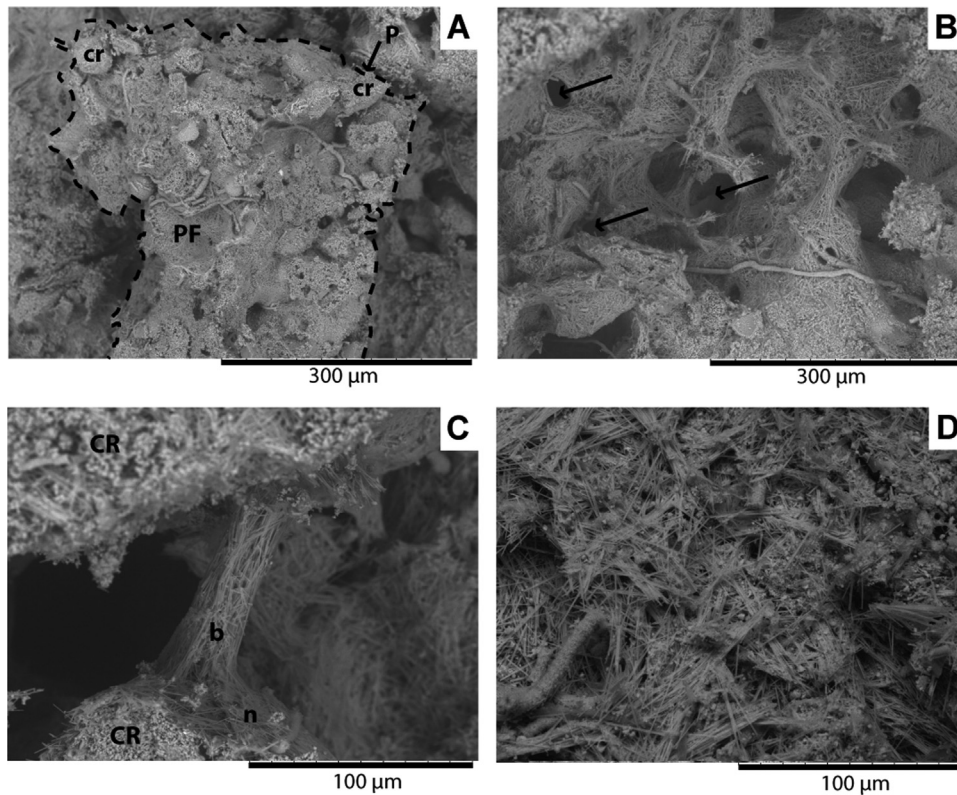The skeleton grains of QCP mainly consist of chalk cryoclasts. These cryoclasts exhibit two main morphologies:

Fig. 4. Microstructures of the CAH and the QCP observed with SEM. Views of A: ped (P) containing small chalk cryoclasts (cr); B: star-shaped vugh that exhibits pore access radii (arrows); C: calcite needle bridge (b) within the intrapedal curved plane between large chalk cryoclasts (CR) coated with calcite needle layer (n) and D: calcite needle disorganized mass in the CAH chamber.

- large chalk cryoclasts ($\varnothing > 0.5$ mm) exhibit circular to ovoid shapes. They can show a well-defined outline or a clear alteration pellicle (Fig. 3A and Fig. 5, cr);
- small chalk cryoclasts ($200\,\mu m < \varnothing < 600\,\mu m$) also exhibit circular to ovoid shapes, but their outline is not clearly defined (Fig. 3B and Fig. 5, CR).

The spatial distribution of cryoclasts is that of a random basic distribution pattern. Their color ranging from white to beige is due to their chalky nature and their alteration intensity. The skeleton of QCP and CAH also shows to a lesser extent Aeolian-originated quartz ($10\,\mu m < \varnothing < 600\,\mu m$), feldspar grains ($10\,\mu m < \varnothing < 50\,\mu m$), and some occurrences of glauconite ($40\,\mu m < \varnothing < 60\,\mu m$).

The plasmic fabric is mainly composed of calcite, which is represented by residual micrite and sparitic and/or microsparitic cements. It also contains a clay assemblage (illite, smectite, and illite/smectite mixed-layer clays). The plasmic fabric exhibits some inorganic residues of biological origin: coccoliths, foraminifers, and shells (fossil biological origin). The color of the plasmic fabric is dark beige to brown. The plasmic fabric appears in two forms:

- it is first systematically composed of a thin coating (20–50 μm) around large chalk cryoclasts (Fig. 3A and Fig. 4, n);
- it is also composed of spheroidal to blocky peds (Soil Survey Staff, 1993) exhibiting a mean diameter of 2 mm,

some of them being 3 mm wide. These peds contain the major part of the small chalk cryoclasts (Figs. 3B, Fig. 4A, and Fig. 5).

Large chalk cryoclasts and spheroidal to blocky peds constitute the macrofeatures of the QCP. These macrofeatures are partially accommodated or unaccommodated and highly to moderately separated (Bullock et al., 1985). This arrangement defines two major types of voids:

- interpedal curved planes (Stoops, 2003), which are about 60 μm large and display numerous constrictions (Fig. 3A; B and C and Fig. 5);
- star-shaped vughs (Stoops, 1998) with a mean diameter of 3 mm. Some secondary spheroidal peds (Bullock and Murphy, 1976) can be found inside star-shaped vughs. These peds have a diameter ranging from 10 to 500 μm. Star-shaped vughs can also can contain some small chalk cryoclasts. However, QCP star-shaped vughs exhibit high values of macroporosity (Fig. 3E, Fig. 4B and Fig. 5).

The entire pore walls are lined with acicular calcite coating approximately 13 μm thick (Fig. 3A, Fig. 4B and Fig. 5). Calcite needles have a length of 10–100 μm and a diameter smaller than 2 μm. Their size and their pairwise association allow us to classify them in the smooth paired rods category: MA1 (Verrecchia and Verrecchia, 1994).

GENERAL MICROMORPHOLOGY
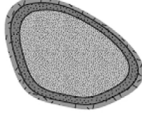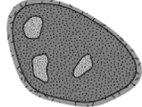
Quaternary cryoturbated paleosol (QCP)   Carbonate accumulation horizon (CAH)
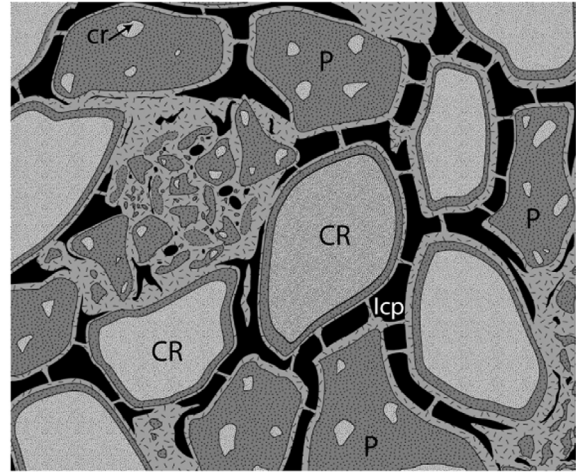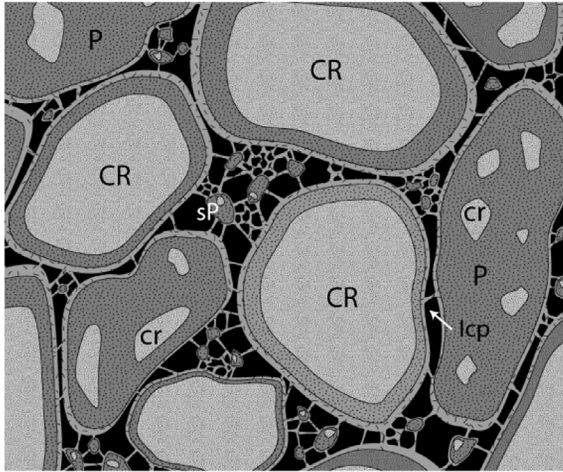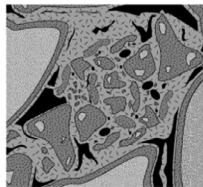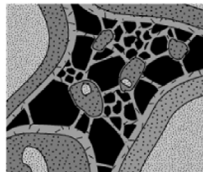

- **MAIN COMPONENTS**

- Chalk
- Plasmic fabric (PF)
- Calcite needles (random arrangement)
- Visible voids on thin sections
- Arch-shaped calcit needles bridges (b)

- **MACROFEATURES**

Large chalk cryoclast (CR) with thin coating of plasmic fabric

Spheroidal to blocky ped (P) with small cryoclasts occurrences (cr) and secondary peds (sP)

- **VOIDS**

STAR SHAPED VUGHS   INTERPEDAL CURVED PLANES

QCP
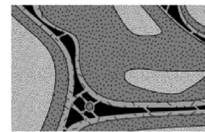
CAH
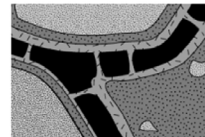
Fig. 5. Schematic representation of the QCP and CAH micromorphologies.

This needle fiber calcite is also agglomerated to form arch-shaped bridges over the voids (Fig. 3A, Fig. 4C and Fig. 5), and thus can exceptionally shrink the star-shaped vughs.

The CAH exhibits the same types of macrofeatures, voids, and calcite needle coating. However, the distribution and the size of these features show some differences, which allow us to characterize the singularity of the CAH (Table 2). The spheroidal to blocky peds within the CAHs exhibit a smaller diameter than in the QCP (800 μm to 1.5 mm). Moreover, they are not systematically well defined unlike the peds observed in the QCP. Interpedal curved planes of the CAH are larger than in the QCP (width up to 140 μm) and are generally well connected, contrary to what is observed in the QCP (Fig. 3D and Fig. 5). The

Table 2
Differences observed between QCP and CAH macrofeatures, voids, and calcite needles.

	QCP	CAH
Macrofeatures		
Large chalk cryoclasts	Ø > 0.5 mm; circular to ovoid shape; well-defined outline or a clear alteration pellicle; thin coating of plasmic fabric (20–50 μm thick)	
Spheroidal to blocky peds	Well defined; Ø: 2–3 mm; relatively uniform size	Nonsystematically well-defined; Ø: 800 μm to 1.5 mm
Voids		
Interpedal curved planes	60 μm mean thick; numerous constrictions	Up to 140 μm mean thick; well connected
Star-shaped vughs	Ø: 3 mm; high macroporosity content	Ø: 6 mm (exceptionally 8 mm); high microporosity content
Calcite needles arrangement	Coating of 13 μm thick on the entire pore walls	
	Numerous arch-shaped bridges in interpedal curved planes and star-shaped vughs	Clearly less disordered aggregates in star-shaped vughs

mean star-shaped vughs observed in the CAH are about two times larger than those present in the QCP (6 mm) (Fig. 3F and Fig. 5). Moreover, some occurrences exhibit a diameter reaching up to 8 mm. As in the QCP, CAH star-shaped vughs present arch-shaped bridges of calcite needles. However, calcite needles form less disordered aggregates (Fig. 4D and Fig. 5).

3.5. Pore system geometry

Total porosity by mercury intrusion (N_{Hg}) obtained on the CAH is $51.6 \pm 5.0\%$. These values of N_{Hg} are significantly higher than that of QCP and chalk samples (respectively 41.0 ± 3.4 and $42.3 \pm 0.2\%$).

Regarding the pore access distribution given by the spread of MIP curves, CAH is highly heterogeneous. No dominant pore access radius could be distinguished, but there was rather a large range of pore access radii from micro- to macroporosity (Fig. 6A). This heterogeneity is reflected by the high values of C_d, i.e. 8.5 ± 4.7.

All the porosimetric curves of QCP are characterized by two well-defined pore access families also present in CAHs, but better defined in QCP (Fig. 6B). The access radii of these two pore families are centered on 0.26 μm for the first one and 30.79 μm for the second one. The corresponding C_d obtained for QCP is 3.3 ± 1.8.

The chalk porosimetric curve shows a unique and very well-defined mode centered on 0.33 μm (Fig. 6C) close to one of the pore families identified in QCP and CAH. The calculated dispersion coefficient C_d is 0.6 ± 0.1.

4. Discussion

CAHs colorimetric characterization is rarely discussed in the specific literature specialized on this type of horizons (e.g., Alonso-Zarza and Wright, 2010; Wright and Tucker, 1991). The macroscopic structures of Champagne-Ardenne CAHs and QCPs are relatively identical on the field, and so the distinction between these two horizons is sometimes difficult. The colorimetric study carried out in the $L^*a^*b^*$ color space shows that CAHs exhibit higher L^* than QCPs, possibly because of a higher total carbonate content. However, the L^* difference between CAHs and QCPs is less important than those observed between QCPs/CAHs and the

rendic leptosol and the chalk. This explains why it is sometimes difficult to identify clearly.

QCPs result from the periglacial alteration of the chalk (Durand, 1979; Loisy and Pascal, 1998). The formation of this type of paleosol is synchronous with the formation of decalcification clay minerals (Harris and Ellis, 1980; Matsuoka, 2001); this could account for higher Al_2O_3 and SiO_2 contents than in the CAHs and chalk. Higher clay mineral contents could explain the redder and yellower tints of QCPs compared to those of the other horizons. As for the rendic leptosol, its redder and yellower tints could be explained by high organic matter content.

If the distinction between CAHs and QCPs is sometimes difficult to the naked eye on the field, the ΔE^* calculation (which takes into account the three $L^*a^*b^*$ colorimetric parameters) shows that CAHs and QCPs distinction can be supported by colorimetric measurement. It is however important to bear in mind that this kind of study is dependent on soil humidity.

Also, for the first time, a penetrometric study carried out here was done with a view to characterizing CAHs within a soil profile. Dynamic penetrometry tests performed through the depth of the soil profile depth show that notwithstanding the carbonate precipitations that they present, CAHs exhibit a low induration that is directly linked to high total porosity values (51.6%). These new data seem to contradict the ideas generally advanced in the literature, which usually defines CAHs as being hard levels (only Durand (1979) nuances this by qualifying CAHs as irregularly cemented). However, induration is not characteristic of CAHs compared to other horizons, and finally, it is not a means by which CAHs can be identified within the soil profile. The absence of a well-discernible characteristic signature of CAHs in the soil profile also does not allow the use of a dynamic penetrometer as a CAHs prospecting method in the soil of Champagne as Maquaire et al. (2002) did within the badlands of the Draix research catchments in order to estimate and map the large spatial variations in the thickness of weathered marl profile.

Previous micromorphological studies focused solely on CAHs levels in order to understand their formation modes (Durand, 1979; Loisy and Pascal, 1998; Loisy et al., 1999). The comparison with other levels of soil profiles (especially QCPs) permits to show that differences exist between CAHs
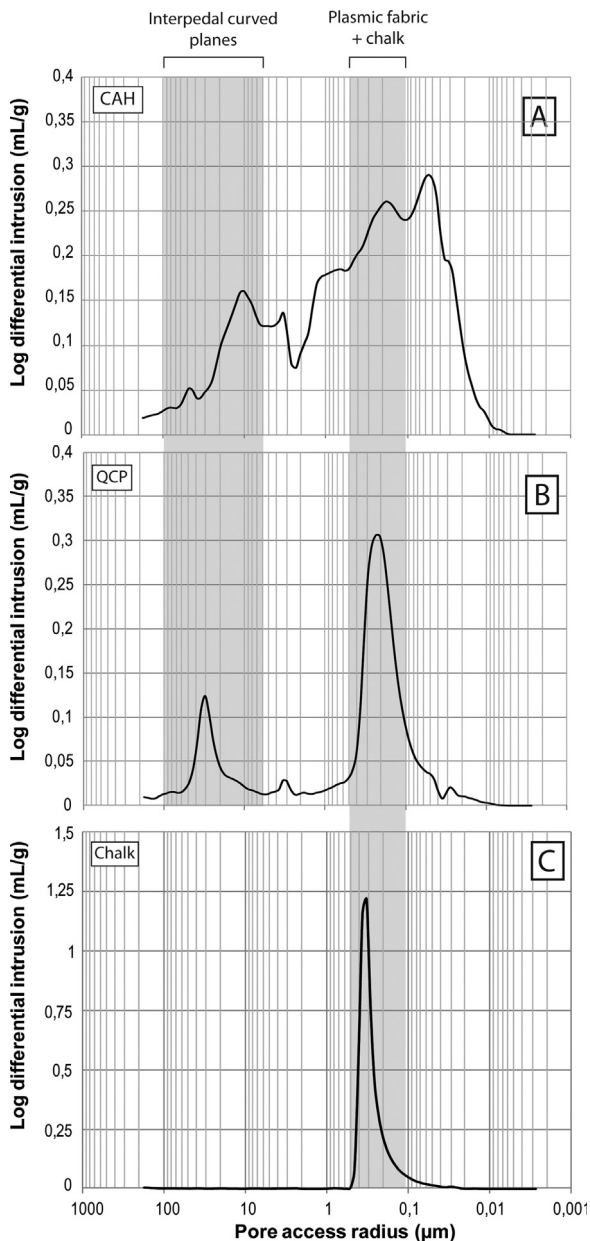
Fig. 6. Mercury intrusion porosimetry curves for (A) Carbonate Accumulation Horizons (CAHs), (B) Quaternary Cryoturbated Paleosol (QCP) and for the chalk (C).

and QCPs. Although CAHs and QCPs present the same micromorphologic entities and void types, the morphological variations of these entities are responsible for the structural differences between CAHs and QCPs.

Mercury intrusion porosimetry curves obtained on QCPs showed a bimodal trend with pore access families ranging between 24.6 and 30.8 μm and between 0.21 and 0.26 μm. Compared to the thin section observations, the first pores family was related to the voids accessible by the interpedal curved planes. The second pore family is too small to correspond to a type of voids observed on thin sections. Some similarities were found between this pore

family (Fig. 4B) with the monomodal repartition of the pore access radii of chalk, typically characterized by a pore mean value of 0.33 μm (which corresponds to the spaces between the coccoliths; Price et al., 2000). This pore family also corresponds to the microporosity of the plasmic fabric and the disordered aggregates of needle fiber calcite.

Within the QCPs, the second family (0.21–0.26 μm) is more extensive and takes into account the internal porosity of the plasmic fabric in addition to the porosity of chalk cryoclasts. On the contrary, the mercury intrusion porosimetry curves of the CAHs generally exhibit plurimodal porous network marked by a dispersion coefficient (C_d) greater than those of the QCP curves (around 10). As in the QCPs, the interpedal curved planes observed in thin sections are visible on CAH mercury intrusion porosimetry curves. However, they cover more important pore access radii intervals. In thin sections, CAH interpedal curved planes exhibit fewer constrictions than in the QCPs. This network included interpedal curved planes and intraparticle pores similar to those found in QCPs. If CAHs resulted from a modification of the QCPs, the presence of such voids may be inferred from the genetic relationship between these two horizons. However, the two horizons showed important differences in pores system with regard to interpedal curved planes and star-shaped vughs. These porosities are more prevalent and more connected in the CAHs than in the QCPs. Access radii affiliated to QCP interpedal curved planes and star-shaped vughs are also observed on CAHs mercury intrusion porosimetry curves. QCP porosimetric signature is recognizable in the CAHs and both horizons show the same micromorphologic entity types. These two new observations tend to confirm the hypothesis of Loisy (1997), who describes the CAH establishment within the QCPs.

It is clearly admitted that calcite needles (NFC) have a biologic origin (Cailleau et al., 2009; Loisy et al., 1999; Verrecchia and Verrecchia, 1994). Although calcite needles are also some of CAH and QCP ubiquitous micromorphological entities, they are much more numerous and appear less clearly organized in star-shaped vughs of the CAHs than in those of the QCPs. This CAHs' characteristic is found in their mercury injection porosimetry curves by the spread of the pore access family to low values.

Microscopic observations coupled with the mercury injection porosimetry and the study of CAHs in their global context within the soil profile allow us to see that the CAHs have present characteristics inherited from their host formations (QCPs). However, their deposition allows them to acquire their own characteristics. Because an important part of these characteristics is relative to porous networks, it is possible to predict that CAHs have an important role within the soil profiles of Champagne. CAHs may indeed induce a more important drainage of the rendic leptosol and the porous network differences between horizons. Moreover, they will induce the presence of hydraulic discontinuity at the soil profiles scale and maybe a lateralization of lateral water transfers.

5. Conclusion

Carbonate accumulation horizons (CAHs) are particular types of horizons deposited within some soil profiles of

Champagne-Ardenne (Northeast of France). When present, these levels of carbonate redistribution are located in the top part of Quaternary cryoturbated paleosols (QCPs) and under the organomineral horizon. Although direct discrimination on the field can be quite difficult, the comparison of CAH characteristics to the other horizons of the soil profiles analyzed in this study showed that CAHs have their own characteristics. This study showed that field colorimetric measurements can be used to identify CAHs and particularly to discriminate them from QCPs. Even though the literature suggests that CAHs have a strong induration, and hence the usual qualification of "crusts," the dynamic penetrometer tests showed that they are not characterized by high hardness compared to other horizons of the soil profiles. This low induration is connected with the very high total porosity they present. Thus, this nondestructive method cannot be used to indicate the presence of CAHs. The study also shows that if CAHs have the porosimetric signature of their host material (QCP) and the same major types of micromorphological features, they differ by a singular structure and heterogeneity of the porous networks. This study highlighted that CAHs exhibit a unique nature within the soil profiles of Champagne. It is an essential first step that will allow the study in greater detail of the impact of CAHs on water transfers or lateral fluxes into the Champagne soil profile.

Acknowledgements

References

Allouc, J., Le Roux, J., 1995. Mourmelon-le-Grand (133), Cartes géol. France (1/50000) BRGM, Orléans.

Allouc, J., Le Roux, J., 2000. Suippes (159), Cartes géol. France (1/50000) BRGM, Orléans.

Alonso-Zarza, A.M., 1999. Initial stages of laminar calcrete formation by roots: examples from the Neogene of central Spain. Sediment. Geol. 126, 177–191.

Alonso-Zarza, A.M., Wright, V.P., 2010. Calcretes. In: Alonso-Zarza, A.M., Tanner, L.H. (Eds.), Developments in Sedimentology. Elsevier, (Chapter 5), pp. 225–267.

Ballantyne, C.K., Harris, C., 1994. The Periglaciation of Great Britain. Cambridge University Press.

Ballif, J.-L., 1994. Etude pédo-agronomique de nouvelles parcelles du domaine du lycée agricole de la Marne. Ferme de la Poste à Somme-Vesle. Carte des sols du domaine, Travaux de la station d'agronomie de Châlons-sur-Marne. INRA Éditions, Châlons-sur-Marne, France, 11 p.

Ballif, J.-L., Guérin, H., Muller, J.-C., 1995. Éléments d'agronomie champenoise ; connaissances des sols et de leur fonctionnement ; rendzines sur craie et sols associés ; esquisse géomorphopédologique. INRA Éditions, Versailles, France.

Banwart, S., Menon, M., Bernasconi, S.M., Bloem, J., Blum, W.E.H., Maia de Souza, D., Davidsdotir, B., Duffy, C., Lair, G.J., Kram, P., Lamacova, A., Lundin, L., Nikolaidis, N.P., Novak, M., Panagos, P., Ragnarsdottir, K.V., Reynolds, B., Robinson, D., Rousseva, S., de Ruiter, P., van Gaans, P., Weng, L., White, T., Zhang, B., 2012. Soil processes and functions across an international network of Critical Zone Observatories: Introduction to experimental methods and initial results. C. R. Geoscience 344 (11–12), 758–772.

Bouttemy, R., 1966. Craonne 3/4-7/8, Asfeld-la-Ville 1/2-5/6. Service de Cartographie des sols de la chambre d'agriculture de l'Aisne, Laon, France.

Bruand, A., Creuzot, G., Quétin, P., Darthout, R., Raison, L., Courtemanche, P., Gaillard, H., 1997. Variabilité de la recharge de la nappe de Beauce. Étude et Gestion des Sols 4 (4), 229–245.

Bullock, P., Murphy, C., 1976. The microscopic examination of sub-surface horizon of soils. Outlook Agric. 8, 348–354.

Bullock, P., Fedoroff, N., Jongerius, A., Stoops, G., Tursina, T., Babel, U., 1985. Handbook for Soil Thin Section Description. Wane Research Publications, Wolverhampton, United Kingdom, 152 p.

Cailleau, G., Verrecchia, E.P., Braissant, O., Emmanuel, L., 2009. The biogenic origin of needle fibre calcite. Sedimentology 56, 1858–1875.

Cérépi, A., Loisy, C., Burlot, R., 2009. Monitoring of water and heat transfer in the vadose zone of a carbonate formation: an example of an underground quarry in Gironde, France. C. R. Geoscience 341, 473–485.

Chéry, P., Lavialle, O., Bourennane, H., King, D., Bruand, A., 1999. Variabilité verticale de la composition granulométrique des limons de Patite Beauce (France). Étude et Gestion des Sols 6 (4), 185–196.

Durand, R., 1979. La pédogenèse en pays calcaire dans le Nord-Est de la France. Université Louis-Pasteur, Strasbourg, 198 p.

Durand, R., 1980. Variations saisonnières de la concentration des solutions et des gaz du sol en milieu crayeux. Science du Sol 3, 217–230.

FAO, IUSS, ISRIC, 2006. World Reference Base for Soil Resources 2006: A Framework for International Classification, Correlation and Communication. Food and Agriculture Organization of the United Nations, Rome.

Gallé, C., 2001. Effect of drying on cement-based materials pore structure as identified by mercury intrusion porosimetry – a comparative study between oven-, vacuum-, and freeze-drying. Cem. Concr. Res. 31, 1467–1477.

Goudie, A.S., 1973. Duricrusts in Tropical Landscape. Clarendon Press, Oxford, UK.

Hamidi, E.M., Colin, F., Michard, A., Boulangé, B., Nahon, D., 2001. Isotopic tracers of the origin of Ca in a carbonate crust from the Middle Atlas, Morocco. Chem. Geol. 176, 93–104.

Harris, C., Ellis, S., 1980. Micromorphology of soils in solifucted materials, Okstindan, northern Norway. Geoderma 23, 11–29.

Hildenbrand, A., Urai, J.L., 2003. Investigation of the morphology of pore space in mudstones–first results. Mar. Pet. Geol. 20, 1185–1200.

Hommeril, P., Martin, P., Puissegur, J.-J., 1974. Les nappes alluviales de la Seine à Cléon (près de Rouen) et leurs intercallations saumâtres. Bull. Assoc. fr. Étude du Quaternaire 11 (3–4), 202–207.

Laurain, M., Guérin, H., Barta, L., Monciardini, C., Allouc, J., 1981. Reims (158), Cartes géol. France (1/50000) BRGM, Orléans, France.

Laurain, M., Guérin, H., Marre, A., Richard, J., 1995. Processus génétiques à l'origine des formations de pente à graviers de craie en Champagne. Permafr. Periglac. Process. 6, 103–108.

Lauriol, B., Clark, I., 1999. Fissure calcretes in the arctic: a paleohydrologic indicator. Appl. Geochem. 14, 775–785.

Loisy, C., 1997. Les encroûtements carbonatés quaternaires en substrat crayeux (Est du bassin de Paris) : rôles de la diagenèse et des actions biologiques. Université de Reims Champagne-Ardenne, Reims, France, 387 p.

Loisy, C., Pascal, A., 1998. Indurated carbonate horizon in chalky Champagne: function of diagenesis and biological effects under temperate climate. Les encroûtements carbonatés (« calcrètes ») en Champagne crayeuse: rôles de la diagenèse et des actions biologiques sous climat tempéré 169, 189–201.

Loisy, C., Verrecchia, E.P., Dufour, P., 1999. Microbial origin for pedogenic micrite associated with a carbonate paleosol (Champagne, France). Sediment. Geol. 126, 193–204.

Maquaire, O., Ritzenthaler, A., Fabre, D., Ambroise, B., Thiery, Y., Truchet, E., Malet, J.-P., Monnet, J., 2002. Caractérisation des profils de formations superficielles par pénétrométrie dynamique à énergie variable: application aux marnes noires de Draix (Alpes-de-Haute-Provence, France). C. R. Geoscience 334, 835–841.

Matsuoka, N., 2001. Solifluction rates, processes and landforms: a global review. Earth-Sci. Rev. 55 (1–2), 107–134.

Moreau, C., 2008. Vieillissement en milieu naturel de pierres calcaires hydrofugées : évaluation de la durabilité des traitements et de leur impact sur le nettoyage. Université de Reims Champagne-Ardenne, Reims, 377 p.

Murton, J.B., Bateman, M.D., Baker, C.A., Knox, R., Whiteman, C.A., 2003. The Devensian periglacial record on Thanet, Kent, UK. Permafr. Periglac. Process. 14, 217–246.

Nicoullaud, B., Darthout, R., Duval, O., 1995. Etude de l'enracinement du blé tendre d'hiver et du maïs dans les sols argilo-limoneux de petite Beauce. Étude et Gestion des Sols 2 (3), 183–200.

Ould Mohamed, S., Bruand, A., 1993. Morphology and origin of secondary calcite in soils from Beauce, France. In: Ringrose-Voase, A.J., Humphreys, G.S. (Eds.), Developments in Soil Science. Elsevier, pp. 27–36.

Price, M., Low, R.G., McCann, C., 2000. Mechanisms of water storage and flow in the unsaturated zone of the Chalk aquifer. J. Hydrol. 233, 54–71.

Remy, J.M., 1993. Influence de la structure du milieu poreux carbonaté sur les transferts d'eau et les changements de phase eau-glace. Application à la durabilité au gel de roches calcaires de Lorraine, Institut national polytechnique de Lorraine, Nancy, 327 p.

Robert, M., Saugier, B., 2003. Contribution des écosystèmes continentaux à la séquestration du carbone. C. R. Geoscience 335, 577–595.

Sanglerat, G., 2012. The Penetrometer and Soil Exploration. Elsevier Science.

Schlesinger, W.H., 1985. The formation of caliche in soils of the Mojave Desert, California. Geochim. Cosmochim. Acta 49, 57–66.

Soil Survey Staff, 1993. Soil Survey Manual, Department Of Agriculture, United States of America. Governmental Printing Office, Washington DC, 503 p.

Spanneut, B., 1997. Tourbe eau pure, fonctionnement hydrogéologique du bassin versant de la Tourbe. Rapport d'activités de la chambre d'agriculture de la Marne, 24.

Stoops, G., 2003. Guideline for analysis and description of soil and regolith thin sections. Soil Science Society of America, Inc., Madison, WI, USA.

Stoops, G., 1998. Key to the ISSS "Handbook for Soil Thin Section Description". Natuurwet. Tijdschrift. 78, 193–203.

Verrecchia, E.P., Verrecchia, K.E., 1994. Needle-fiber calcite; a critical review and a proposed classification. J. Sediment. Res. 64, 650–664.

Wardlaw, N.C., McKellar, M., Li, Y., 1988. Pore and throat size distribution determined by mercury porosimetry and by direct observations. Carbonates Evaporites 3 (1), 1–15.

Wright, V.P., Tucker, M.E., 1991. Calcretes: an introduction. In: Wright, V.P., Tucker, M.E. (Eds.), Calcretes. Blackwell Scientific Publications, Oxford, pp. 1–22.

Yven, B., Sammartino, S., Géraud, Y., Homand, F., Villiéras, F., 2007. Mineralogy, texture and porosity of Callovo-Oxfordian argillites of the Meuse/Haute-Marne region (eastern Paris basin). Mem. Soc. geol. France 178, 73–90.